

Environmental Science Processes & Impacts

Accepted Manuscript



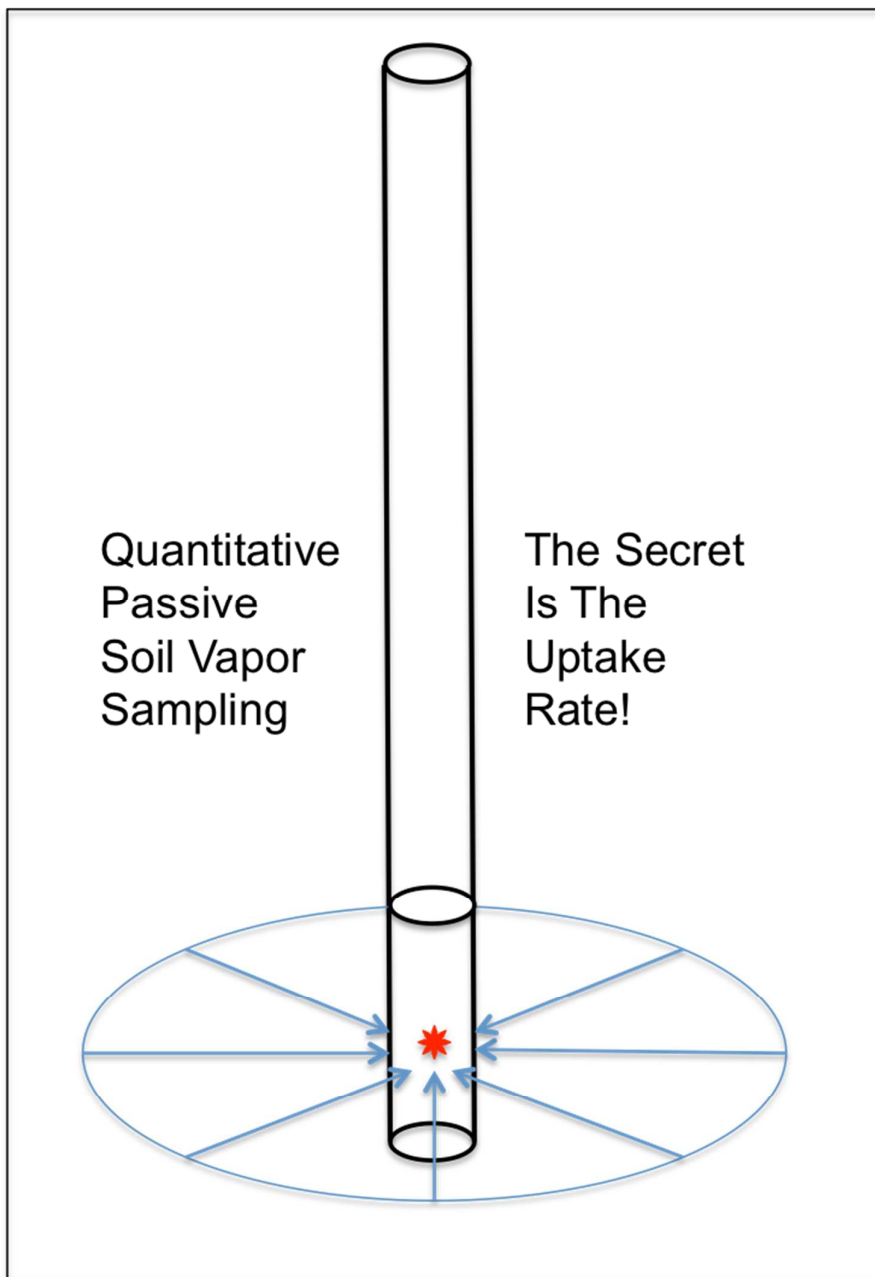
This is an *Accepted Manuscript*, which has been through the Royal Society of Chemistry peer review process and has been accepted for publication.

Accepted Manuscripts are published online shortly after acceptance, before technical editing, formatting and proof reading. Using this free service, authors can make their results available to the community, in citable form, before we publish the edited article. We will replace this *Accepted Manuscript* with the edited and formatted *Advance Article* as soon as it is available.

You can find more information about *Accepted Manuscripts* in the [Information for Authors](#).

Please note that technical editing may introduce minor changes to the text and/or graphics, which may alter content. The journal's standard [Terms & Conditions](#) and the [Ethical guidelines](#) still apply. In no event shall the Royal Society of Chemistry be held responsible for any errors or omissions in this *Accepted Manuscript* or any consequences arising from the use of any information it contains.

Table of Contents Entry



Environmental Impact Statement

To accompany the submission of the draft paper entitled: Quantitative Passive Soil Vapor Sampling for VOCs – Part 1: Theory

McAlary et al, 2013

Conventional soil vapor sampling for VOC analysis can be time-consuming if quality control measures are implemented to verify the absence of leaks and sample collection may be impractical in low-permeability soils. Passive adsorptive sampling has been an alternative to conventional active sampling for decades, but the uptake rate of the sampler has never been well understood or controlled, so passive sampling has been considered a qualitative or semi-quantitative method. This paper provides a theoretical framework using a combination of steady-state and transient mathematical models to support an improved design for passive diffusive samplers for soil vapor monitoring, which minimizes the starvation effect, maximizes the sensitivity and provides quantitative concentration measurements for a wide range of soil types.

Quantitative Passive Soil Vapor Sampling for VOCs: Theory

Todd McAlary^{1,3*}, Xiaomin Wang², Andre Unger², Hester Groenevelt¹, Tadeusz Górecki³

¹ Geosyntec Consultants, Inc. 130 Research Lane, #2, Guelph, Ontario, N1G 5G3

² Department of Earth and Environmental Sciences, University of Waterloo, Waterloo, Ontario
Canada

³ Department of Chemistry, University of Waterloo, Waterloo, Ontario Canada

ABSTRACT

Volatile organic compounds are the primary chemicals of concern at many contaminated sites and soil vapor sampling and analysis is a valuable tool for assessing the nature and extent of contamination. Soil gas samples are typically collected by applying vacuum to a probe in order to collect a whole-gas sample, or by drawing gas through a tube filled with an adsorbent (active sampling). There are challenges associated with flow and vacuum levels in low permeability materials, and leak prevention and detection during active sample collection can be cumbersome. Passive sampling has been available as an alternative to conventional gas sample collection for decades, but quantitative relationships between the mass of chemicals sorbed, the soil vapor concentrations, and the sampling time have not been established. This paper presents transient and steady-state mathematical models of radial vapor diffusion to a drilled hole and considerations for passive sampler sensitivity and practical sampling durations. The results indicate that uptake rates in the range of 1 to 0.1 mL/min will minimize the starvation effect for most soil moisture conditions and provide adequate sensitivity for human health risk assessment with a practical sampling duration. This new knowledge provides a basis for improved passive soil vapour sampler design.

*Corresponding Author - phone: (519) 822-2230 ext 239; fax (519) 822-3151; e-mail: tmcalary@geosyntec.com

23

24 INTRODUCTION

25 Knowledge of the spatial distribution of volatile organic compound (VOC) vapors in the
26 subsurface is essential for assessing human health risks associated with subsurface vapor
27 migration and intrusion to indoor air, as well as for monitoring the performance of related
28 mitigation and remediation systems (sub-slab venting, soil vapor extraction, multiphase
29 extraction, air sparging, bioventing, etc.). There are a wide variety of different methods and
30 guidance available for soil vapor sampling and analysis^{1,2,3,4,5,6,7,8}, but few comparative studies
31 that evaluate the relative performance between various active soil vapor sampling methods⁹.
32 Currently, the most common method for collection and analysis of sub-slab or soil vapor samples
33 during vapor intrusion investigations in North America (and to varying degrees elsewhere) is an
34 active method whereby soil gas is drawn into an evacuated, passivated stainless steel container
35 (e.g., SilcoTek™ SilcoCan® or Summa® canisters) through a flow controller, followed by
36 shipment to a laboratory for analysis by EPA Method TO-15¹⁰. Sampling protocols for canisters
37 are complicated because subsurface permeabilities and soil vapor concentrations can both vary
38 over many orders of magnitude and care is needed to prevent and document the absence of leaks
39 of atmospheric air into the sample train¹¹. Passive sampling does not involve applying a vacuum
40 to draw a volume of gas as a sample, and with no induced pressure gradient, the potential for low
41 bias attributable to leakage is dramatically reduced or eliminated.

42 At the present time, there are varying opinions regarding the reliability of soil vapor sampling for
43 assessing human health risks posed by VOCs. For example, the ITRC vapor intrusion guidance⁶
44 states: “Soil gas data are recommended over other data, specifically soil matrix and groundwater
45 data, because soil gas data represent a direct measurement of the contaminant that can potentially
46 migrate into indoor air”. However, the empirical database of soil vapor and indoor air

47 concentrations compiled by the USEPA¹² shows a worse correlation between soil vapor and
48 indoor air VOC concentrations than the corresponding comparison between groundwater and
49 indoor air VOC concentrations. It is not clear what role sampling errors or biases play in the
50 relatively poor correlation between soil vapor and indoor air concentrations; however, protocols
51 using passive sampling devices are considerably simpler than active sampling protocols, and
52 simpler protocols are likely to reduce variability attributable to operator error, which provides an
53 incentive to advance the science of passive soil vapor sampling.

54 Passive sampling is an alternative approach with several potential advantages over conventional
55 whole-gas sampling, including simpler protocols, smaller size for ease of shipping and handling,
56 and lower overall cost (including the labor cost for sample collection). Much of the historic
57 application of passive sampling has been indoor and outdoor air quality monitoring and
58 industrial hygiene applications^{13,14,15,16,17}. Several passive soil gas sampling methods have been
59 developed over the past quarter century since the earliest efforts¹⁸, including Petrex tubes^{19,20},
60 EMFLUX® cartridges²¹, Beacon B-Sure Sample Collection Kits™²² and Gore™ Modules
61 (formerly known as the Gore-Sorber®)²³. Each of these methods provides results in units of the
62 mass adsorbed over the duration of the sample; however, the correlation between the mass
63 adsorbed and the soil vapor concentration has not been quantitatively established^{24,21,23}.
64 Concentration values are needed for comparison to risk-based screening levels when assessing
65 human health risks via vapor intrusion, so many regulatory guidance documents caution that
66 passive soil gas sampling should only be used as a qualitative or semi-quantitative screening
67 tool^{24,25}. Overcoming this limitation was the primary motivation of this research.

68 **THEORY**

69 Quantitative passive samplers are of two general varieties: equilibrium samplers (where the
70 sampler equilibrates with the surrounding medium), and kinetic samplers (where the sampler is
71 designed to have a constant uptake rate throughout the sample duration). This paper deals
72 exclusively with kinetic passive samplers because the focus of this research was human health
73 risk assessment associated with subsurface vapour intrusion to indoor air, where time-weighted
74 average concentrations are preferred.

75 The basic principles of operation for quantitative passive samplers are as follows. Each device is
76 supplied by the laboratory certified clean and sealed in air-tight packing. The sampler is exposed
77 to the air or soil gas being investigated for a measured amount of time (t), during which VOCs
78 diffuse or permeate into the device from the surrounding gas or air in response to the chemical
79 potential (i.e. concentration) gradient²⁶. A certain mass of VOCs is trapped by the sorptive
80 medium within the device. After sampling, the device is shipped in an air-tight container to the
81 analytical laboratory, where the mass sorbed is quantified. The time-weighted average (TWA)
82 concentration (c) of a particular analyte in the medium being sampled is then calculated as
83 follows²⁶:

$$84 \quad c = \frac{Mk}{t} \quad (1)$$

85 where:

86 c = TWA concentration of a particular analyte in the sampled air [$\mu\text{g}/\text{m}^3$]

87 M = mass of analyte on the sorbent, blank-corrected if needed [pg]

88 k = calibration constant [min/mL]

89 t = sampling time [min]

90 (note that there are two offsetting conversion factors from pg to μg and mL to m^3)

91 The reciprocal of the calibration constant ($1/k$) is referred to as the uptake rate (UR), which has
92 units of mL/min. Even though the uptake rate has units of [volume/time], it is important to

93 emphasize that it does not represent a real flow; rather, it is simply a number equivalent to the
94 flow that would produce the same mass loading on an active adsorptive sampler that had air
95 pulled through it for the same c and t . The mass adsorbed and the sample duration can both be
96 measured very accurately (commonly within 5% to 15%), so the accuracy of the uptake rate is
97 the key factor controlling the accuracy of the calculated concentration. Quantitative kinetic
98 passive samplers are designed to control the uptake rate of chemicals during sampling using
99 well-defined barriers between the sorbent and the media being sampled of a fixed cross-sectional
100 area and known diffusion or permeation characteristics for the chemicals of interest. The uptake
101 rates of kinetic samplers are typically measured in controlled exposure chamber experiments or
102 calculated from first principles based on the free-air diffusion coefficient or permeation rate of
103 the particular compound of interest^{27,28,29,30,31,32,33}.

104 High uptake rates allow lower concentrations to be quantified with shorter sample durations,
105 which can be an advantage in some instances. Lower uptake rates reduce the risk of the
106 “starvation effect”, which occurs when the rate-limiting step is transport of chemicals to the
107 sampler instead of the uptake rate of the sampler itself. This situation results in a reduction in
108 vapor concentrations near the sampler, and a negative bias in the calculated passive sampler
109 concentrations compared to the conditions under which the passive sampler uptake rate was
110 measured. Advection from wind and ventilation during indoor and outdoor air sampling is often
111 sufficient to minimize or eliminate the starvation effect completely. For soil gas sampling,
112 advection is likely to be minimal and the rate of contaminant vapor replenishment in the gas-
113 filled void space surrounding the sampler is likely to be dominated by diffusive transport, which
114 is the focus of the mathematical models presented in this paper. The uptake rate of a passive
115 sampler can be increased or decreased by design, and the calculations presented here support the
116 selection of appropriate uptake rates for quantitative passive soil vapor sampling.

117 **Conceptual Model For Quantitative Passive Soil Vapor Sampling**

118 Passive soil vapor sampling is usually performed by drilling a hole in the ground, removing soil,
119 placing a passive sampler in the void-space created by drilling, sealing the hole from the
120 atmosphere for the duration of the sample, then retrieving the sampler and backfilling or grouting
121 the hole. A simple conceptual model of this scenario is as follows:

- 122 • Immediately after the hole is drilled and the soil is removed, the void space fills with air.
123 Assuming atmospheric air can enter the void space with less resistance than gas flowing
124 through the surrounding soil, the initial concentration of vapors inside the void space
125 would be expected to be much lower than that in the surrounding soil, and at worst could
126 be assumed to be essentially zero (if atmospheric air is contaminant-free).
- 127 • In most cases, passive samplers are placed in the borehole and the space above the
128 sampler is sealed without purging to remove atmospheric air from the void space around
129 the sampler (purging is feasible during passive soil vapor sampling, but not common).
- 130 • During the period of sampling, vapors diffuse into the void space from the surrounding
131 soil. If the void space is long relative to its diameter and short enough that the geologic
132 properties and vapor concentrations are relatively uniform over the vertical interval of the
133 void space, then the diffusion will be essentially radially symmetric (this has been
134 assumed for the remainder of this paper).
- 135 • The rate of diffusive mass transport into the void space over time will depend on the
136 concentration gradient and effective diffusion coefficient, and will gradually diminish as
137 the concentration in the void space increases toward equilibration with the surrounding
138 soil. If a passive sampler is present in the void space, the concentration in the void space
139 will remain somewhat below the concentration in the surrounding soil depending on the
140 uptake rate of the passive sampler.

- 141 • If the uptake rate of the sampler is small relative to the rate of diffusion into the void
142 space (a goal if the starvation effect is to be small), then the steady-state concentration in
143 the void space will be similar to the concentration in the surrounding soil and passive
144 sampling will be able to provide a quantitative measure of the soil vapor concentration.

145 **Mathematical Modeling of Quantitative Passive Sampling**

146 Passive soil vapor sampling involves transport of vapors through the soil surrounding the
147 drillhole into the void space in which the sampler is deployed, diffusion through the air inside the
148 void-space, and uptake by the sampler. The free-air diffusion coefficient through the air inside
149 the void space will be roughly one to several orders of magnitude higher than the effective
150 diffusion coefficient in the surrounding soil, so vapor transport through the air inside the void
151 space is not expected to be the rate-limiting step. This allows the mathematical analysis to focus
152 on two components: the rate of vapor diffusion into the void space (the “diffusive delivery rate”,
153 or DDR) and the rate of vapor uptake by the passive sampler (“passive sampler uptake rate” or
154 UR). Understanding the rate of diffusion of vapors into the void space is necessary to design an
155 uptake rate for the passive sampler that is low enough to minimize the starvation effect.
156 However, the uptake rate must also be high enough to provide adequate sensitivity (ability to
157 meet target reporting limits with an acceptable sampling duration), so both constraints must be
158 considered.

159 **Influence of Soil Moisture on the Effective Diffusion Coefficient in Soil**

160 The effective diffusion coefficient depends strongly on the total porosity (volume of pores
161 divided by total volume of soil) and water-filled porosity (volume of water divided by total
162 volume of soil, otherwise known as the volumetric water content). Understanding this
163 relationship is helpful for context in the theory of passive soil gas sampling if diffusion is the

164 main process delivering vapors to the void space in which the sampler is deployed. Johnson and
165 Ettinger³⁴ adopted the Millington-Quirk³⁵ equation in their well-known model for assessing the
166 potential for subsurface vapor intrusion to indoor air. Their formulation of the effective diffusion
167 coefficient also includes diffusion in the aqueous phase, assuming the Millington-Quirk
168 empirical relationship is equally valid for both the gas and water phases:

$$D_{eff} = D_{air} \frac{\theta_a^{10/3}}{\theta_T^2} + \frac{D_w}{H} \frac{\theta_w^{10/3}}{\theta_T^2} \quad (2)$$

170 where the parameters are defined in Table 1. Parameter values used for all calculations in this
171 paper were selected to be representative of trichloroethene (TCE), one of the most common
172 VOCs of interest for human health risk assessment associated with contaminated land. Many
173 other VOCs have similar diffusion coefficients and Henry's Law constants, so the general trend
174 applies for a range of VOCs of interest for human health risk assessments. Equation (2) was used
175 to calculate D_{eff} for both the transient and steady-state models in this paper.

176 TABLE 1

177 A series of calculations were performed using Equation (2) and the parameter values in Table 1
178 to show the relationship between the effective diffusion coefficient and the water-filled porosity.
179 The calculated D_{eff} values span a range from about 0.01 to about 0.00001 cm²/s over a range of
180 water-filled porosities from 1% to 36% in a soil with 36% porosity (Figure 1). These values are
181 indeed much lower than the free-air diffusion coefficient (0.069 cm²/s), which supports the
182 assumption that diffusion through the air in the void space in which the sampler is deployed is
183 not rate-limiting.

184 FIGURE 1

185 Two models (transient and steady-state) are presented to simulate the passive sampling process.

186 TRANSIENT MODEL

187 The conceptualization for a transient mathematical model of radial diffusion of vapors from soil
 188 into the void space is shown in Figure 2. For simplicity, the transient model simulates an empty
 189 void space (i.e, no passive sampler), which is a reasonable approximation because a passive
 190 sampler with an uptake rate low enough to minimize the starvation effect would only become
 191 significant as the concentration inside the void space approached steady-state. The derivation of
 192 the transient model is provided in Supplemental Information. In summary, the governing
 193 equations are:

194 Concentration in the gas phase within the void space $c_g(r, t)$;

$$\frac{\partial c_g}{\partial t} - D_{air} \left[\frac{\partial^2 c_g}{\partial r^2} + \frac{1}{r} \frac{\partial c_g}{\partial r} \right] = 0 \quad 0 \leq r < r_2 \quad (3)$$

195 Concentration in the soil vapor surrounding the void space $c_s(r, t)$;

$$\frac{\partial c_s}{\partial t} - D_{eff} \left[\frac{\partial^2 c_s}{\partial r^2} + \frac{1}{r} \frac{\partial c_s}{\partial r} \right] = 0 \quad r_2 \leq r < r_3 \quad (4)$$

196 The initial and boundary conditions are also shown in Figure 2. A Laplace transform is applied
 197 to convert the partial differential equations into ordinary differential equations and other
 198 operations are performed as described in the Supplemental Information to obtain:

$$\bar{c}_g = \frac{c_{s0}}{p} \frac{\varphi_2}{\varphi_2 \varphi_4 - \varphi_1 \varphi_3 \varphi_5} \left[\frac{K_1(q_g r_1)}{I_1(q_g r_1)} I_0(q_g r) + K_0(q_g r) \right] \quad (5)$$

$$\text{for } 0 \leq r < r_2$$

199

$$\bar{c}_s = \frac{c_{s0}}{p} + \kappa \frac{c_{s0}}{p} \frac{\varphi_2}{\varphi_2 \varphi_4 - \varphi_1 \varphi_3 \varphi_5} \frac{\varphi_1 \varphi_3}{\varphi_2} \left[\frac{K_1(q_s r_3)}{I_1(q_s r_3)} I_0(q_s r) + K_0(q_s r) \right] \quad (6)$$

$$\text{for } r_2 \leq r < r_3$$

200 Equations (7) and (8) allow the calculation of the mass in the void space based on the mass flux
 201 across the borehole wall from the void side and soil side, respectively.

$$\bar{M}(p) = \frac{D_{air}c_{s_0}}{p^2} q_g \frac{\varphi_2}{\varphi_2\varphi_4 - \varphi_1\varphi_3\varphi_5} \left[\frac{K_1(q_g r_1)}{I_1(q_g r_1)} I_1(q_g r_2) - K_1(q_g r_2) \right] \quad (7)$$

$$= \frac{D_{air}c_{s_0}}{p^2} q_g \frac{\varphi_2\varphi_1}{\varphi_2\varphi_4 - \varphi_1\varphi_3\varphi_5}.$$

$$\bar{M}(p) = \frac{D_s c_{s_0}}{p^2} q_s \frac{\varphi_2}{\varphi_2\varphi_4 - \varphi_1\varphi_3\varphi_5} \frac{\varphi_1\varphi_3}{\varphi_2} \left[\frac{K_1(q_s r_3)}{I_1(q_s r_3)} I_1(q_s r_2) - K_1(q_s r_2) \right] \quad (8)$$

$$= \frac{D_s c_{s_0}}{p^2} q_s \frac{\varphi_2\varphi_1\varphi_3}{\varphi_2\varphi_4 - \varphi_1\varphi_3\varphi_5}.$$

202 The inverse Laplace transforms of Equation (5), (6), (7) and (8) are computed numerically using
 203 the algorithm developed by DeHoog et al.³⁷. The modified Bessel functions I_α and K_α used for
 204 Equations (5), (6), (7) and (8) are defined by:

$$I_\alpha(x) = i^{-\alpha} J_\alpha(ix) = \sum_{m=0}^{\infty} \frac{1}{m! \Gamma(m + \alpha + 1)} \left(\frac{x}{2}\right)^{2m+\alpha} \quad (9)$$

205

$$K_\alpha(x) = \frac{\pi I_{-\alpha}(x) - I_\alpha(x)}{2 \sin(\alpha\pi)} = \frac{\pi}{2} i^{\alpha+1} H_\alpha^{(1)}(ix) = \frac{\pi}{2} (-i)^{\alpha+1} H_\alpha^{(2)}(-ix) \quad (10)$$

206 The meaning of the symbols in the equations is explained in the Supplementary Information.

207 **FIGURE 2**

208 **STEADY-STATE MODEL**

209 If the duration of passive sampling is long compared to the time required for the vapor
 210 concentrations in the void space to approach equilibrium with the surrounding soils, then a
 211 steady-state model would also provide insight into the passive sampling mechanisms. For this
 212 case, the conceptual model is as follows:

- 213 • The vapor concentration in the soil surrounding the void space is uniform at c_s beyond a
 214 radial distance of r_3 ,
- 215 • Diffusion occurs in the region between the outer wall of the drillhole (radius = r_2) and r_3 ,

216 through a cylinder of height, h ,

- 217 • The concentration in the gas inside the void space of the borehole (c_g) is lower than c_s by
- 218 a factor $\delta = c_g/c_s$ (this value should be close to 1.0 in order for the sampler to be exposed
- 219 to vapor concentrations very similar to the surrounding soil),
- 220 • Radial diffusion occurs from the soil to the void space at a diffusive delivery rate equal to
- 221 the passive sampler uptake rate for the majority of the sample deployment interval (i.e.,
- 222 the sampling period is long compared to the time required for steady-state diffusion to be
- 223 established).

224 The rate of mass transfer (R_{MT}) of vapors into the borehole via vapor diffusion through the

225 surrounding soil (R_{MT1}) is given by Carslaw and Jaeger (1959):

$$226 \quad R_{MT1} = \frac{2\pi h D_{eff} (C_s - C_g)}{\ln\left(\frac{r_3}{r_2}\right)} \quad (11)$$

227 The rate of mass uptake by the sampler (R_{MT2}) is given by:

$$228 \quad R_{MT2} = c_g \times UR \quad (12)$$

229 Setting $R_{MT1} = R_{MT2}$ gives:

$$230 \quad UR \left[\frac{mL}{min} \right] = \frac{2\pi h [cm] D_{eff} \left[\frac{cm^2}{s} \right] (1-\delta)}{\ln\left(\frac{r_3}{r_2}\right) \delta} \times 60 [s/min] \quad (13)$$

231 RESULTS AND DISCUSSION

232 TRANSIENT MODEL SIMULATIONS

233 A series of simulations were performed using the transient model to show the relationship

234 between the mass entering the void space from the surrounding soil and time for a 2.54 cm (1-

235 inch) diameter drillhole, a soil vapor concentration (c_s) of $100 \mu\text{g}/\text{m}^3$ and a vertical interval of 10

236 cm. Figure 3 shows simulations for a variety of different water-filled porosities (θ_w) and the

237 corresponding effective diffusion coefficients calculated using Equation 2. For all water contents

238 simulated, the mass of TCE in the void space eventually reaches the same steady value as the
239 concentration inside the void space equilibrates with the surrounding soil. These simulations are
240 instructive because they indicate the time required for the void space to equilibrate with the
241 surrounding soil as a function of the moisture content. For relatively dry soils (e.g., $\theta_w < 0.1$), the
242 void space concentration would be within 10% of the soil vapor concentration in as little as about
243 10 minutes. For wet soils (e.g., $\theta_w = 0.30$), a similar level of equilibration may require up to
244 about 1 day.

245 **FIGURE 3**

246 Equilibration occurs more slowly with larger diameter boreholes. A comparison of the
247 equilibration time for a nominal 1-inch and 4-inch diameter voids of 10 cm height are shown in
248 Table 2, which shows that the difference in equilibration time is proportional to the difference in
249 the volume of the void space (i.e., varies in proportion to the square of the borehole radius). Most
250 passive samplers can fit within a borehole of 2-inch diameter or less, so the equilibration time
251 would be less than 1 day for most soil moisture contents.

252 **TABLE 2**

253 The transient model simulations do not account for mass removed by a passive sampler in the
254 borehole, which would draw a small but not insignificant amount of mass from the surrounding
255 soil over time. At steady-state, the uptake rate of the passive sampler (UR) and the diffusive
256 delivery rate from the surrounding soil (DDR) would be equal; therefore, Equation (1) can be re-
257 arranged to:

$$258 \quad DDR = \frac{M}{C t} \quad (14)$$

259 In the period of time before steady-state is achieved, the diffusive delivery rate (DDR) would not
260 be constant and equal to the uptake rate of the sampler, rather, it would be high initially when the
261 concentration gradient is the largest, and gradually slow down as the concentration inside the

262 void space equilibrates with the surrounding soil. Equation 14 can be used to calculate DDR
263 values as a function of time where M is calculated using Equation 8 for a given period of time (t)
264 and a c_s value of $100 \mu\text{g}/\text{m}^3$, as shown in Figure 4. The DDR diminishes to less than about 1
265 mL/minute within about 30 minutes for all moisture contents. Quantitative passive samplers for
266 indoor air quality monitoring typically have uptake rates of 10 to 100 mL/min^{27,28,29,30,31,32,33}, so
267 these simulations demonstrate that a customized sampler with a lower uptake rate would be
268 needed to minimize the starvation effect to enable reliable quantitative soil vapor sampling for all
269 but very short sample durations and dry soils.

270 **FIGURE 4**

271 The DDR decreases as the concentration in the void space approaches equilibrium with the
272 surrounding soil vapor, as shown in Figure 5. For very dry soils, the average DDR is greater than
273 10 mL/min until about 90% of the mass has entered the void-space (which occurs within 10
274 minutes according to Figure 3). In this scenario, a passive sampler with an uptake rate as high as
275 10 mL/min may still provide data with an acceptably small starvation effect. In other words, the
276 sampler uptake rate remains below the diffusive delivery rate from the soil until the mass
277 delivered to the void space is about 90% of the steady-state value, so a negative bias of about
278 10% may be expected, which would meet the data quality objectives typically used for soil vapor
279 monitoring (precision within 25% RPD³⁶). For very wet soils ($\theta_w = 0.30$), the average DDR is
280 about 0.01 mL/min by the time the void space has nearly equilibrated with the surrounding soil
281 (roughly 1 day). For moisture contents typical of most vadose zone soils ($0.10 < \theta_w < 0.25$),
282 Figure 5 shows that an uptake rate of about 1 mL/min would be expected to result in an
283 acceptably small starvation effect (i.e., for a water-filled porosity of up to 25% in a soil with 36%
284 porosity, the bias due to the starvation effect for a sampler with an uptake rate of 1 mL/min
285 would be expected be less than -20%).

286 **FIGURE 5**287 **Superposition of Diffusive Delivery Rate and Uptake Rate**

288 The transient mathematical model presented in the previous section must be processed further to
289 demonstrate the effect of adding a passive sampler to the void space. A mathematical model
290 including 2-dimensional radial diffusion to the void space (diffusive delivery), 3-dimensional
291 diffusion through the void-space to the passive sampler, and uptake by a variety of possible
292 passive sampler designs and geometries is challenging to formulate mathematically. However, an
293 approximate model can be derived by adding the diffusive delivery rate (Figure 4) and the
294 sampler uptake rate to estimate the effect of both processes occurring at the same time, using the
295 principle of superposition. As long as the uptake rate of the sampler is small, the combined
296 model will differ from the transient analytical model of radial diffusion only after the diffusion
297 into the void space has very nearly attained steady-state, at which time the diffusive delivery rate
298 of vapors into the void space will stabilize at the same value as the uptake rate of the sampler.
299 Figure 6 shows an example of the diffusive uptake rate that would be expected if a passive
300 sampler with an uptake rate of 1 mL/min was placed in the void-space simulated in Figures 3, 4
301 and 5. Within about 1 hour, the delivery rates for all water-filled porosities approach the uptake
302 rate of the sampler (within about a factor of 2). The delivery rate becomes equal to the uptake
303 rate for all soil moisture contents within about 1 day.

304 **FIGURE 6**

305 It should be noted that for very wet soils (water-filled porosity greater than 0.25), the steady-state
306 delivery rate may be less than 1 mL/min, in which case there are two possibilities: 1) a lower
307 uptake rate sampler could be used with a proportionately longer sample duration, or 2) a negative
308 bias attributable to starvation may still be experienced. If the negative bias is predictable or
309 acceptably small, the data may still be useful and this may be reasonably evaluated using the

310 models presented here as long as the porosity and moisture content are known or can be
311 reasonably estimated. From a practical perspective, very wet soils have an effective diffusion
312 coefficient about two orders of magnitude lower than dry soils (Figure 1), which would reduce
313 the risk to human health from subsurface vapor intrusion to indoor air by a similar amount.
314 Therefore, a slight negative bias in the passive sampler result may still result in protective
315 decision-making if the results are compared to screening levels derived to be protective of dry
316 soil conditions. Also, it may be possible to avoid low bias associated with wet soils by design
317 via either: 1) coring the soil and selecting coarse-textured, well-drained intervals for monitoring;
318 2) sampling during dry seasons; or 3) sampling within the rain-shadow below buildings (a.k.a.,
319 sub-slab samples).

320 **STEADY STATE MODEL SIMULATIONS**

321 For a passive sampler deployed in a borehole with a nominal diameter of 1-inch ($r_1 = 1.25$ cm)
322 and sealed within a 10 cm void space ($h = 10$ cm), the uptake rates calculated using Equation
323 (13) are shown in Figure 7 for δ values of 0.5, 0.75 and 0.95. The r_3 value for these calculations
324 was assumed to be 1 m. Figure 7 shows that an uptake rate of 10 mL/min might be acceptable for
325 very dry soil if the data quality objective was to quantify concentrations within a factor of 2 (i.e.,
326 $\delta = 0.5$), however; an uptake rate of 1 mL/min would be more suitable for soils with water-filled
327 porosity of up to about 15%, assuming a more stringent data quality objective of $\pm 25\%$ (i.e., δ
328 $= 0.75$). Progressively lower uptake rates would be required to further reduce the negative bias or
329 meet typical data quality objectives in very wet soils.

330 **FIGURE 7**

331 A sensitivity analysis on the r_3 value is shown in Figure 8 for the same conditions as in Figure 7
332 and a δ value of 0.75. This plot shows that the value assumed for r_3 does not affect the
333 conclusions in a significant way even when it is varied by an order of magnitude.

334 **FIGURE 8**335 **PRACTICAL CONSTRAINTS ON THE UPTAKE RATE**

336 There is a practical lower limit to the uptake rate for passive sampling, which is imposed by the
337 sample duration needed to achieve a specified reporting limit. Equation (1) can be rearranged to
338 calculate the sample duration required to achieve a target reporting limit if the uptake rate of the
339 sampler and the laboratory mass reporting limit (M_{RL}) are known:

$$340 \quad t = \frac{M_{RL}}{c \times UR} \quad (14)$$

341 For example, consider an initial soil vapor concentration of $100 \mu\text{g}/\text{m}^3$ of TCE and a sampler
342 with an uptake rate of $1 \text{ mL}/\text{min}$. A detectable mass of TCE ($M_{RL} \sim 0.05 \mu\text{g}$ via solvent
343 extraction, GC/MS) would be adsorbed by the sampler in 500 min (0.35 day). This demonstrates
344 that a low-uptake rate sampler can provide practical sensitivity within a reasonable amount of
345 time and still avoid or minimize the starvation effect. However, if the uptake rate was reduced to
346 0.1 or $0.01 \text{ mL}/\text{min}$, the sample duration would need to increase to 3.5 or 35 days , respectively.
347 There are logistical challenges with long sample durations (costs of return travel to field sites,
348 security, etc.). The sensitivity can be increased using thermal desorption instead of solvent
349 extraction ($M_{RL} \sim 0.002 \mu\text{g}$); however, weaker sorbents are typically used with thermal
350 desorption, hence less-strongly sorbed analytes may not be effectively retained, especially for
351 longer sampling durations.

352 **CONCLUSIONS**

353 In order for a kinetic passive sampler to provide quantitative soil vapor concentration data, it
354 must have a known and reliable uptake rate for all of the compounds of interest. The passive
355 sampler uptake rate should be low enough to allow the rate of diffusive delivery of vapors into
356 the void space from the surrounding soil to sustain vapor concentrations in the void space similar

357 to those of the surrounding soil in order to minimize the starvation effect. The uptake rate must
358 also be high enough to provide the ability to detect concentrations at or below risk-based
359 screening levels with acceptable sampling duration. This paper demonstrates that kinetic
360 samplers with the uptake rates in the range of ~ 0.01 to ~ 10 mL/min can deliver quantitative
361 passive soil vapor concentration data with only a small bias, depending on the soil moisture, and
362 that an uptake rate of about 1 mL/min provides acceptable accuracy and sensitivity for most
363 commonly-encountered water-filled porosities in unsaturated soils. These conclusions are
364 supported by both transient and steady-state models. The knowledge gained from the
365 mathematical modeling in this paper allows passive samplers to be modified as needed to
366 achieve an uptake rate small enough to minimize starvation and high enough to provide adequate
367 sensitivity, which will simplify and improve the cost-effectiveness of quantitative soil vapor
368 concentration measurement and monitoring for VOCs.

369 **ACKNOWLEDGEMENTS**

370 Funding for this work was provided by the Environmental Security Technology Certification
371 Program (ESTCP) with Sam Brock of the Air Force Civil Engineering Center and Andrea
372 Leeson of ESTCP as the DOD Liaisons and the U.S. Navy SPAWAR Systems Center Pacific
373 with Ignacio Rivera-Duarte and Bart Chadwick as contracting officers, under subcontract to
374 Richard Brady and Associates and Computer Sciences Corporation under the Improved
375 Assessment Strategies for the Vapor Intrusion project, which is funded by the Navy's
376 Environmental Sustainability Development to Integration (NESDI) Program. Co-investigators
377 for the ESTCP project include Paul Johnson (Arizona State University), Derrick Crump
378 (Cranfield University, UK), Paolo Sacco (Fondazione Salvatore Maugeri, Italy), Brian
379 Schumacher (USEPA, Las Vegas), Michael Tuday (formerly of Columbia Analytical Services,
380 Simi Valley, CA), Heidi Hayes (Eurofins/Air Toxics Limited, Folsom, CA) and Suresh

381 Seethapathy (formerly of the University of Waterloo). Thanks also to Robert Ettinger and Chris
382 Neville for input on the mathematical models.
383

384 REFERENCES

- 385 1. ASTM D5314 – 92. *Standard Guide for Soil Gas Monitoring in the Vadose Zone*, ASTM
386 International, West Conshohocken, P.A., www.astm.org, 2006.
- 387 2. ASTM D7663 – 11. *Standard Practice for Active Soil Gas Sampling in the Vadose Zone*
388 *for Vapor Intrusion Evaluations*, ASTM International, West Conshohocken, P.A.,
389 www.astm.org, 2011.
- 390 3. Electric Power Research Institute (EPRI). *Reference Handbook for the Site-Specific*
391 *Assessment of Subsurface Vapor Intrusion to Indoor Air*, EPRI Document #1008492, Palo
392 Alto, CA, March, 2005.
- 393 4. American Petroleum Institute (API). *Collecting and Interpreting Soil Gas Samples from*
394 *the Vadose Zone: A Practical Strategy for Assessing the Subsurface Vapor-to-Indoor Air*
395 *Migration Pathway at Petroleum Hydrocarbon Sites*, API Publication #4741, 2005.
- 396 5. *Direct-Push Installation of Devices for Active Soil Gas Sampling and Monitoring*,
397 Geoprobe® Technical Bulletin #3099, May, 2006.
398 http://geoprobe.com/sites/default/files/pdfs/soil_gas_sampling_and_monitoring_mk3098.pdf
- 399 6. *Vapor Intrusion Pathway: A Practical Guideline*, Interstate Technology and Regulatory
400 Council (ITRC), 2007. <http://www.itrcweb.org/Documents/VI-1.pdf>
- 401 7. *Final Scoping Assessment of Soil Vapor Monitoring Protocols for Evaluation of*
402 *Subsurface Vapor Intrusion to Indoor Air*, Canadian Council of Ministers of the
403 Environment (CCME), PN1427 2009. http://www.ccme.ca/assets/pdf/pn_1427_vapor_scoping1.pdf
- 404 8. *Advisory – Active Soil Gas Investigation*, California Department of Toxic Substances
405 Control (DTSC), Cypress, CA, April 2012.
406 http://www.dtsc.ca.gov/SiteCleanup/upload/VI_ActiveSoilGasAdvisory_FINAL_043012.pdf

- 407 9. *Comparison of Geoprobe® PRT and AMS GVP Soil-Gas Sampling Systems With*
408 *Dedicated Vapor Probes in Sandy Soils at the Raymark Superfund Site*, EPA/600/R/111,
409 November, 2006. <http://permanent.access.gpo.gov/lps85174/600R06111.pdf>
- 410 10. *Compendium of Methods for the Determination of Toxic Organic Compounds in Ambient*
411 *Air, Second Edition*, Compendium Method TO-15 - Determination Of Volatile Organic
412 Compounds (VOCs) In Air Collected In Specially-Prepared Canisters And Analyzed By
413 Gas Chromatography/ Mass Spectrometry (GC/MS), Center for Environmental Research
414 Information Office of Research and Development, U.S. EPA, Cincinnati, OH, January
415 1999, PA, EPA/625/R-96/010b.
- 416 11. T.A. McAlary, P. Nicholson, H. Groenevelt, D. Bertrand, *Groundwater Mon. and Rem.*,
417 2009, 29, 144–152.
- 418 12. *EPA's Vapor Intrusion Database: Evaluation and Characterization of Attenuation Factors*
419 *for Chlorinated Volatile Organic Compounds and Residential Buildings*, Office of Solid
420 Waste, U.S. EPA, Washington, DC 20460 EPA/530-R-10-002, March, 2012.
- 421 13. R.H. Brown, *J. Environ Monit*, 2000, 2, 1-9.
- 422 14. J. Namieśnik, B. Zabiegała, A. Kot-Wasik, M. Partyka, and A. Wasik. *Anal and Bioanal*
423 *Chem* 2005, 381, 279-301.
- 424 15. S. Seethapathy, T. Górecki, X. Li, *J Chromatogr A.*, 2008, 1184, 234-253.
- 425 16. T. Górecki and J. Namiesnik, *Trends in Anal Chem*, 2002, 21(4), 276-291.
- 426 17. D.P. Adley and D.W. Underhill, *Anal. Chem.*, 1989, 61(8), 843-847.
- 427 18. *The Use of Industrial Hygiene Samplers for Soil Gas Measurement*, Environmental
428 Monitoring Systems Laboratory, Office of Research and Development, U.S. EPA,
429 EPA/600/4-89/008, 1988.

- 430 19. D.C. Gomes, M. Alarsa, M.C. Salvador and C. Kupferschmid, *Water Sci. Technol.* 1994,
431 29, 161.
- 432 20. M. Anderson and G. Church, *J. Environ. Eng.* 1998, 124, 555.
- 433 21. *Environmental Technology Verification Report, Soil Gas Sampling Technology, Quadrel*
434 *Services, Inc., EMFLUX Soil Gas System*, U.S. EPA Office of Research and Development.
435 EPA Report No. 600/R-98/096, 1998.
- 436 22. Beacon, 2013. <http://www.beacon-usa.com/services/passive-soil-gas-surveys/>, accessed on
437 December 26, 2013.
- 438 23. *Environmental Technology Verification Report, Soil Gas Sampling Technology, W. L.*
439 *Gore & Associates, Inc. GORE-SORBBER Screening Survey*, U.S. EPA Office of Research
440 and Development. EPA Report No. 600/R-98/095, 1998.
- 441 24. ASTM Standard D7758. *New Practice for Passive Soil Gas Sampling in the Vadose Zone*
442 *for Source Identification, Spatial Variability Assessment, Monitoring and Vapor Intrusion*
443 *Evaluations*, ASTM International, West Conshohocken, PA., www.astm.org, 2011.
- 444 25. *Final Guidance for the Evaluation and Mitigation of Subsurface Vapor Intrusion to Indoor*
445 *Air (Vapor Intrusion Guidance)*, California Environmental Protection Agency/Department
446 of Toxic Substances Control (EPA/DTSC), October 2011.
447 http://www.dtsc.ca.gov/AssessingRisk/upload/Final_VIG_Oct_2011.pdf
- 448 26. T. Górecki, and J. Namiesnik, *Trends in Anal. Chem.*, 2002, 21, 276-291.
- 449 27. S. Batterman, T. Metts and P. Kalliokoski, *J. Environ. Monit.*, 2002, 4, 870–878.
- 450 28. G. Subramamian (Ed.), *Quality Assurance in Environmental Monitoring – Instrument*
451 *Methods, Appendix A*. John Wiley & Sons, 2008, 350.
- 452 29. *Performance of SKC Ultra Passive Sampler Containing Carboxen 1016, Carbotrap Z, or*
453 *Chromosorb 106 When Challenged with a Mixture Containing Twenty of OSHA SLTC's*

- 454 *Top Solvent Analytes*, United States Department of Labor Occupational Safety and Health
455 Administration, Washington, D.C., 2003.
456 http://www.osha.gov/dts/sltc/methods/studies/chrom_106_ultra/chrom_106_ultra.html
- 457 30. V. Cocheo, C. Boaretto and P. Sacco, *Am. Ind. Hyg. Assoc. J.*, 1996, 57, 897-904.
- 458 31. C. Chung, M. Morandi, T. Stock and M. Afshar, *Environ. Sci. Technol.*, 1999, 33, 3666–
459 3671.
- 460 32. S. Seethapathy and T. Górecki, *J Chromatogr A.*, 2011, 1218, 143-155.
- 461 33. S. Seethapathy and T. Górecki, *J Chromatogr A.*, 2010, 1217, 7907-7913.
- 462 34. P. Johnson and R. Ettinger, *Environ. Sci. Technol.* 1991, 23, 1445-1452.
- 463 35. R.J. Millington and R.P. Quirk, *Trans. Farad. Soc.*, 1961, 57, 1200-1207.
- 464 36. California Department of Toxic Substances Control and Regional Water Quality Control
465 Board, 2012. Advisory – Active Soil Gas Investigations, accessed on Nov. 14, 2013.
466 http://dtsc.ca.gov/SiteCleanup/upload/VI_ActiveSoilGasAdvisory_FINAL_043012.pdf
- 467 37. F.R. DeHoog, J.H. Knight and A.N. Stokes, *SIAM J. Sci. Stat. Comput.*, 1982, 3, 357-
468 366.

469 Table 1: Parameter Values used in Model Simulations (representative for TCE)

470

Parameter name	Symbol	Units	Value
Free air diffusion coefficient	D_{air}	cm^2/s	0.069
Aqueous diffusion coefficient	D_{w}	cm^2/s	0.00001
Henry's Law constant	H	dimensionless	0.35
Total porosity	θ_{T}	Volume of voids / total volume of soil	0.375
Water-filled porosity	θ_{w}	Volume of water / total volume of soil	Various values from 0.01 to 0.36
Air-filled porosity	θ_{a}	$\theta_{\text{T}} - \theta_{\text{w}}$	Various values from 0.365 to 0.015

471

472 Table 2: Comparison of time to reach 95% of steady-state concentration in the void space
 473 comparing nominal 1-inch and 4-inch diameter boreholes (total porosity 37.5%)

Water-filled porosity (-)	D_{eff} (m^2/day)	Time to reach 95% C_{s0} (day)		t_4/t_1
		t_1 ($r_2 = 0.5\text{inch}$)	t_4 ($r_2 = 2\text{inch}$)	
0.01	0.15	0.0048	0.076	16
0.05	0.10	0.0070	0.11	
0.1	0.058	0.012	0.19	
0.15	0.030	0.024	0.38	
0.2	0.013	0.055	0.87	
0.25	0.0042	0.17	2.7	
0.3	0.00080	0.87	13	
0.31	0.00052	1.3	21	
0.32	0.00033	2.1	34	
0.33	0.00020	3.5	56	
0.34	0.00013	5.5	88	
0.35	0.000093	7.5	120	
0.36	0.000084	8.3	130	

474

475 Figure 1: Effective diffusion coefficient versus water-filled porosity for TCE in a soil with
476 37.5% total porosity, typical of a sandy soil.

477 Figure 2: Schematic of transient mathematical model domain including boundary and initial
478 conditions

479 Figure 3: Simulated mass delivered by diffusion from surrounding soil to the void space versus
480 time for a 2.5 cm diameter borehole in a sandy soil with 37.5% total porosity and an initial soil
481 vapor concentration of $100 \mu\text{g}/\text{m}^3$, assuming no removal of mass by a passive sampler.

482 Figure 4: Diffusive delivery rate versus time for mass entering the void space of a 2.5 cm
483 diameter, 10 cm tall void space in a soil with 37.5% total porosity and an initial soil vapor
484 concentration of $100 \mu\text{g}/\text{m}^3$, assuming no removal of mass by a passive sampler.

485 Figure 5: Relationship between the instantaneous diffusive delivery rate of vapors into the void
486 space versus the percentage of the analyte mass at steady-state ($100 \times M_t/M_{ss}$, where M_t is the
487 analyte mass in the borehole at time t , and M_{ss} is the analyte mass at steady state), assuming a 2.5
488 cm diameter borehole in a soil with 37.5% total porosity, initial soil vapor concentration of 100
489 $\mu\text{g}/\text{m}^3$, and no removal of mass by a passive sampler.

490 Figure 6: Superimposed diffusive delivery rate plus uptake rate for a 10 cm tall and 2.5 cm
491 diameter void space in a soil with 37.5% porosity and an initial soil vapor concentration of 100
492 $\mu\text{g}/\text{m}^3$ containing a passive sampler with an uptake rate of 1 mL/min.

493 Figure 7: Calculated uptake rate corresponding to various δ values as a function of water-filled
494 porosity for a 10 cm tall and 2.54 cm diameter void space assuming $r_3 = 1\text{m}$

495 Figure 8: Calculated uptake rate corresponding to various r_3 values as a function of water-filled
496 porosity for a 10 cm tall and 2.54 cm diameter void space assuming $\delta = 0.75$.

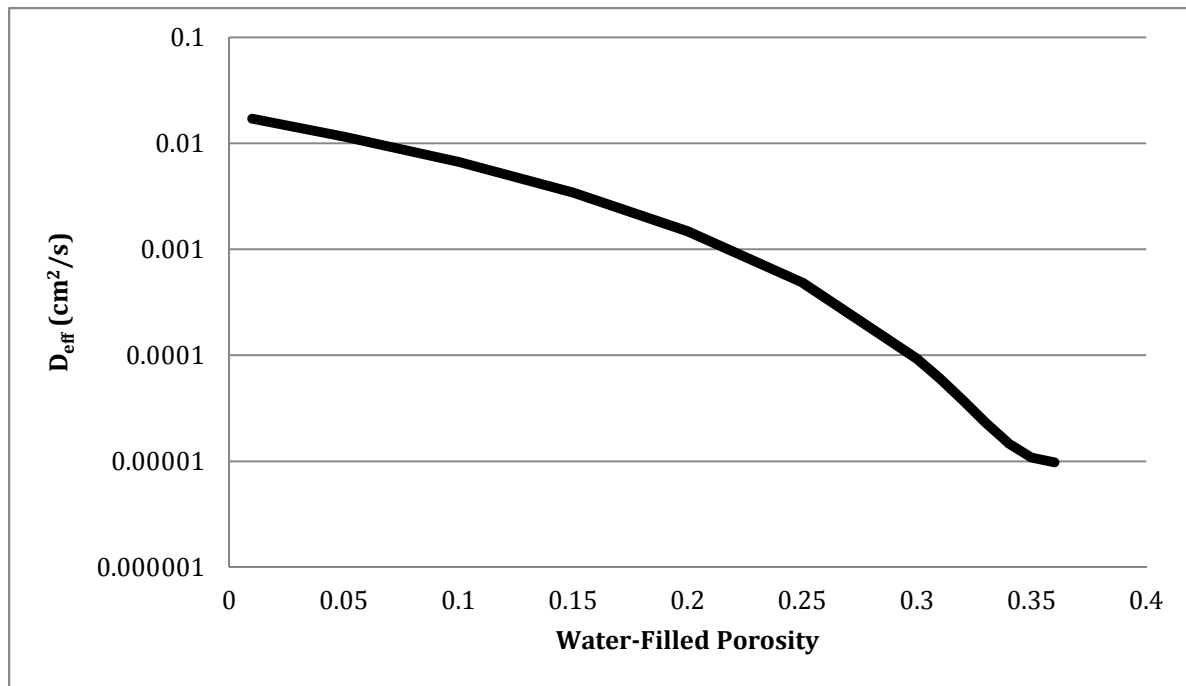
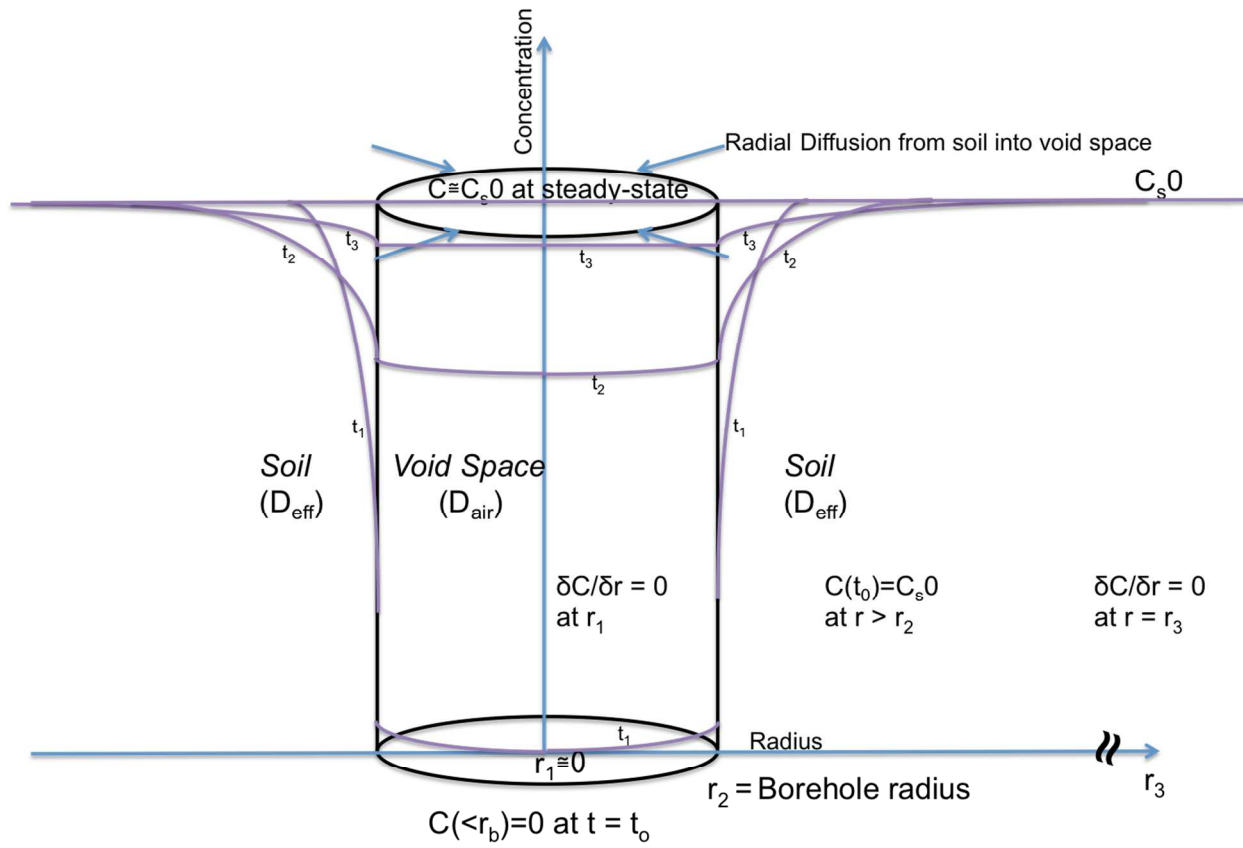


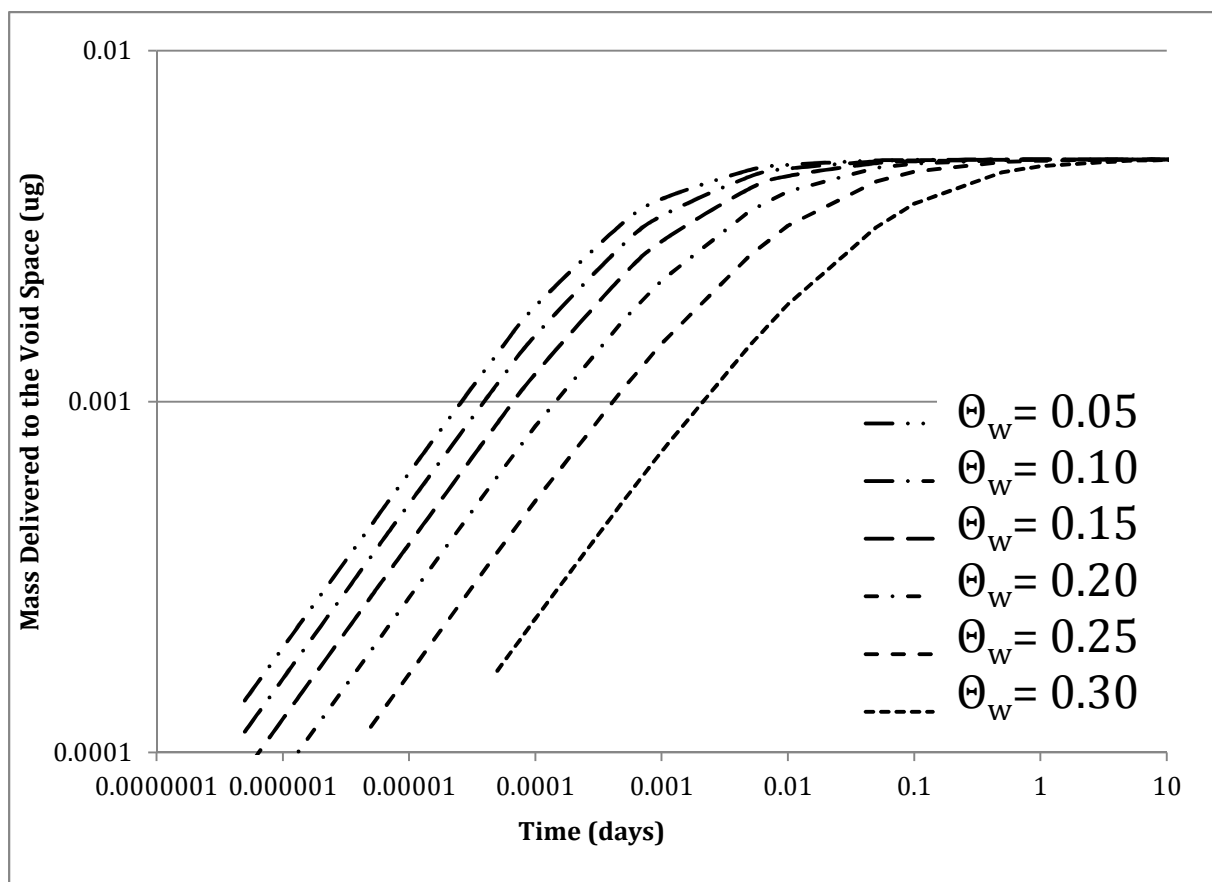
Figure 1

497
498

499

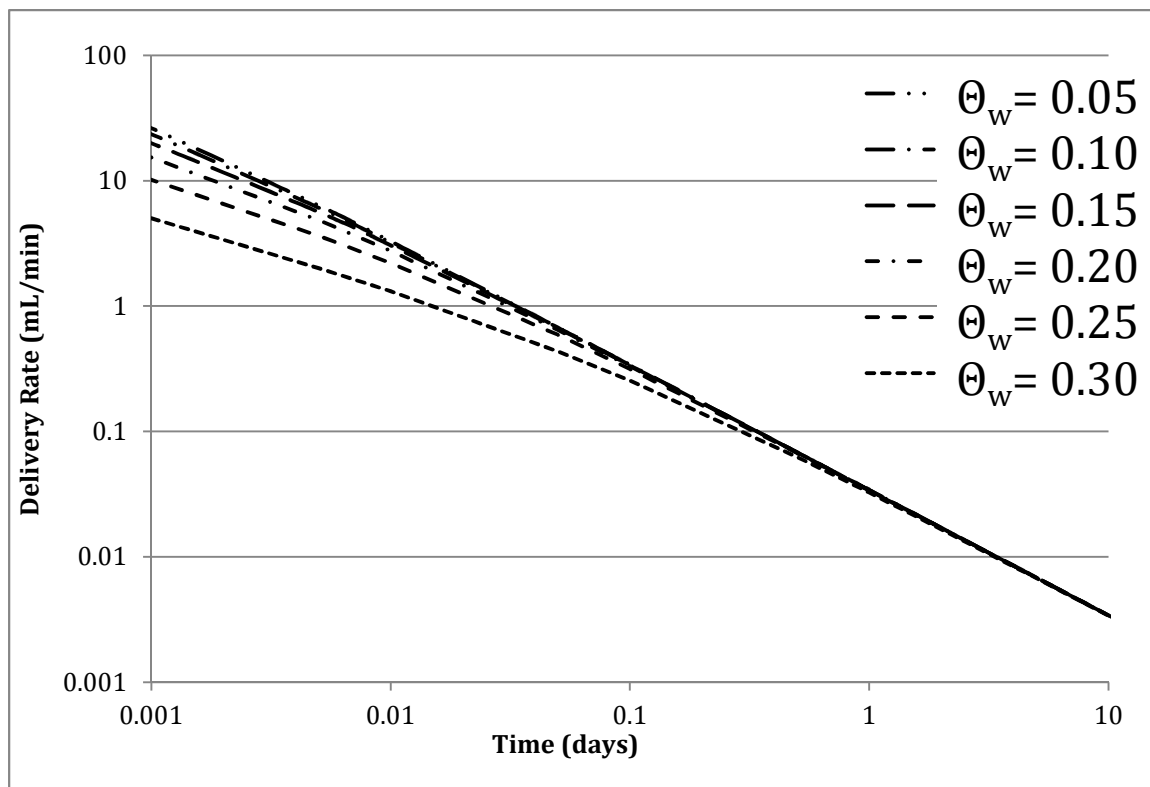


500 Figure 2
501



502

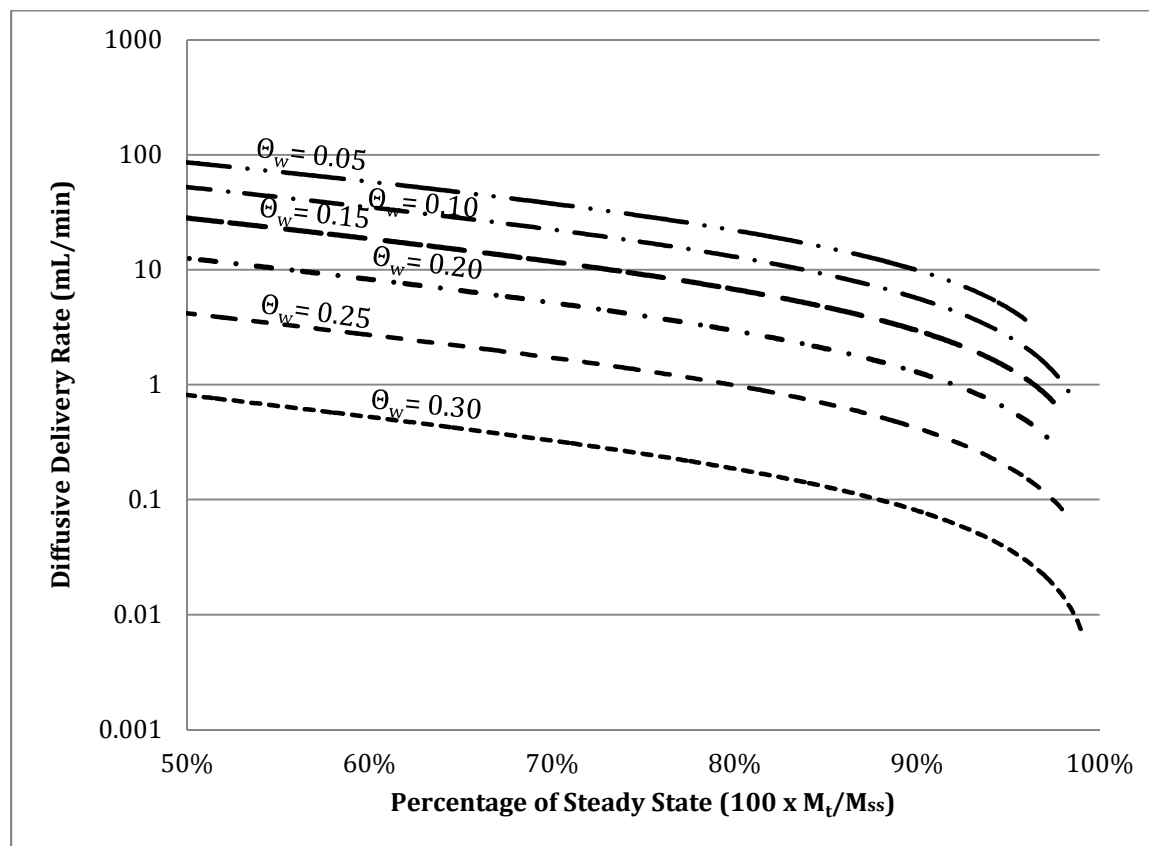
503 Figure 3



504

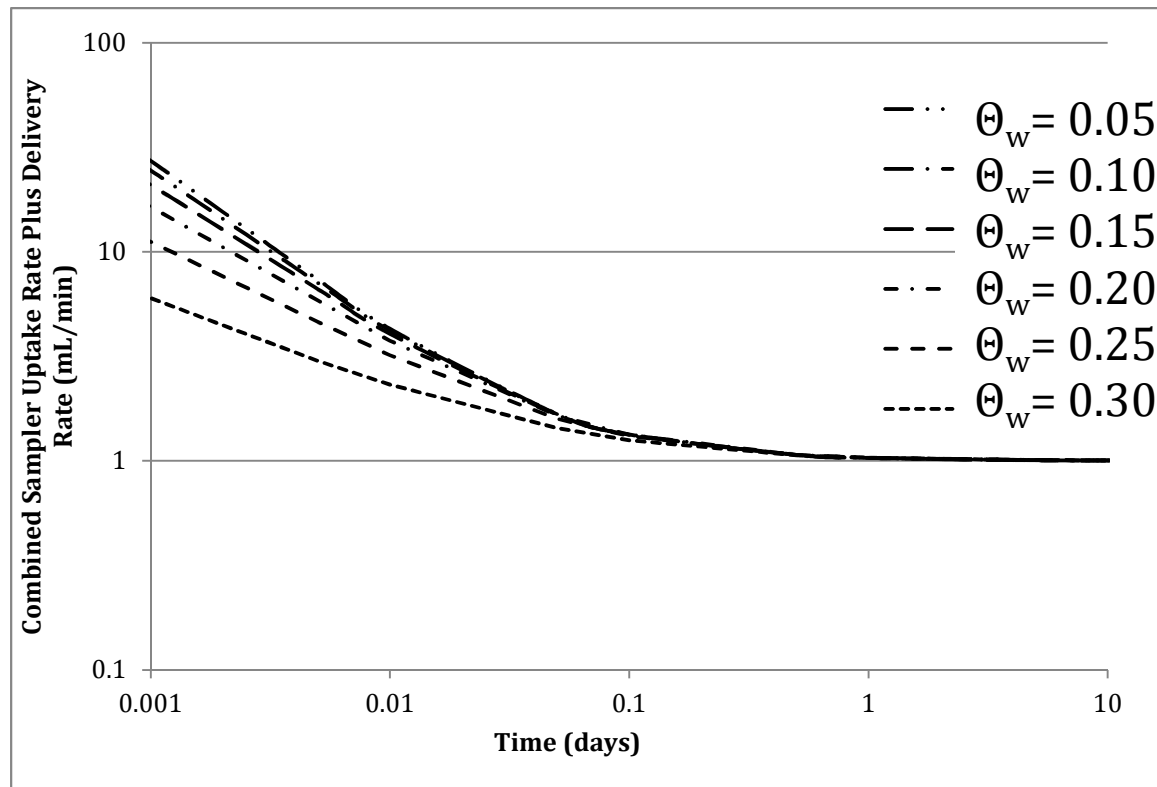
505 Figure 4

506



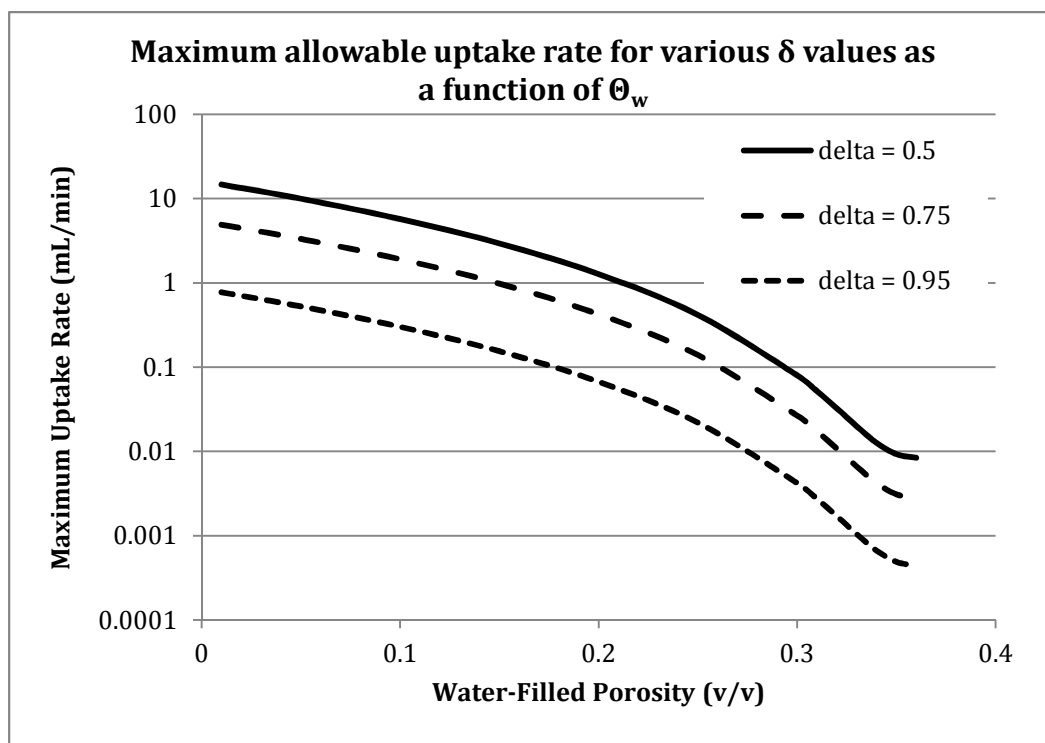
507

508 Figure 5



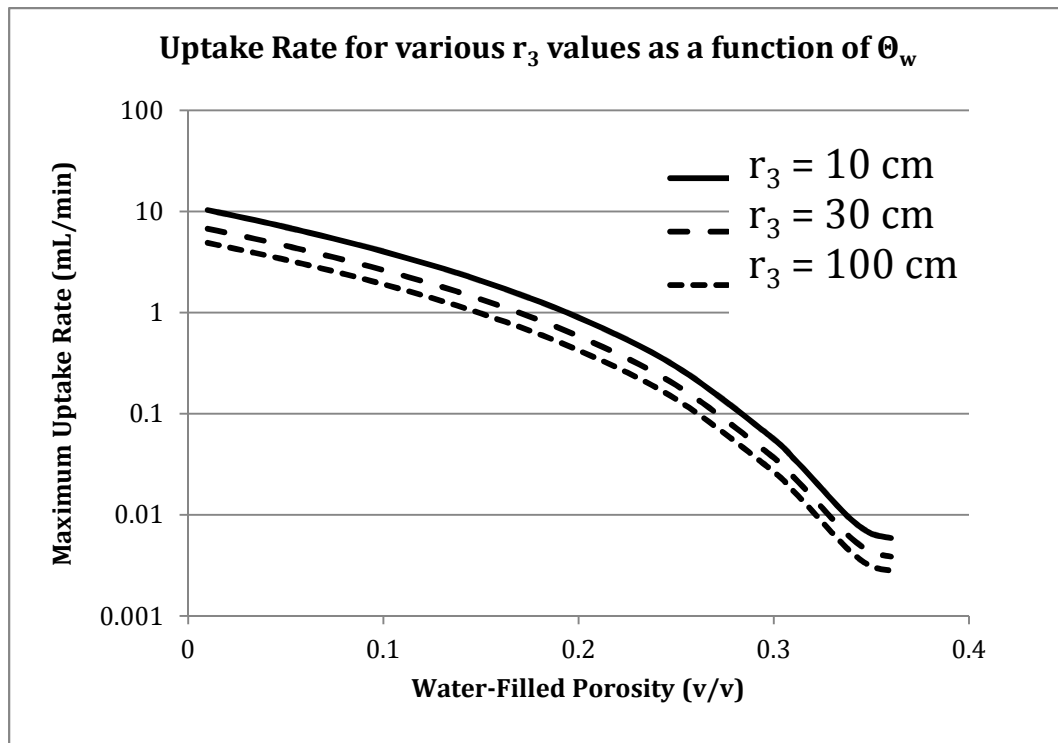
509

510 Figure 6



511

512 Figure 7



513

514 Figure 8

515